

## Transition from laminar to turbulent drag in flow due to a vibrating quartz fork

M. Blažková, D. Schmoranzer, and L. Skrbek

Joint Low Temperature Laboratory, Institute of Physics ASCR and Faculty of Mathematics and Physics, Charles University,  
V Holešovičkách 2, 180 00 Prague, Czech Republic

(Received 5 September 2006; published 9 February 2007)

Flow due to a commercially available vibrating quartz fork is studied in gaseous helium, He I and He II, over a wide range of temperatures and pressures. On increasing the driving force applied to the fork, the drag changes in character from laminar (characterized by a linear drive vs velocity dependence) to turbulent (characterized by a quadratic drive vs velocity dependence). We characterize this transition by a critical Reynolds number  $Re_{cr}^{\delta} = U_{cr} \delta / \nu$ , where  $U_{cr}$  is the critical velocity,  $\nu$  stands for the kinematic viscosity,  $\delta = \sqrt{2\nu/\omega}$  is the viscous penetration depth, and  $\omega$  is the angular frequency of oscillations. We have experimentally verified that the corresponding scaling  $U_{cr} \propto \sqrt{\nu\omega}$  holds in a classical viscous fluid over two decades of  $\nu$ .

DOI: 10.1103/PhysRevE.75.025302

PACS number(s): 47.27.Cn, 47.27.nb, 67.40.Bz, 67.55.Fa

The vibrating quartz tuning fork (Fig. 1) represents an easy to use, robust, cheap, and widely available tool to generate and probe an important class of flows—oscillating boundary layer flows, especially under cryogenic conditions [1]. Commercially produced piezoelectric forks—frequency standards ( $2^{15}=32\,768$  Hz) for watches—are supplied by various producers [2] in a cylindrical vacuum-tight metal can that for fluid dynamical applications has to be entirely or partly removed. In this work, we use them to study one particular feature of an oscillating boundary layer flow—its transition from the laminar to the turbulent drag regime.

The bare fork, its typical surface roughness, and the electrical scheme used for measurements are shown in Fig. 1. The fork is excited with an ac voltage  $U_D = U_0 \cos(\omega t)$ , where  $\omega$  is the angular frequency of oscillations. The observable quantity is a current owing to the piezoelectric effect  $I = aU$  measured by the SR 830 lock-in amplifier, which is proportional to the derivative of the fork deflection, i.e., its velocity  $U$ . For calibration, one needs to find the proportionality constant  $a$ . We use the vacuum measurements of the linewidth  $\Delta\omega$  obtained by slowly sweeping the drive frequency across the resonance at liquid-nitrogen ( $\approx 78$  K) or liquid-helium ( $\approx 4.2$  K) temperature, at which the flow is then probed. As explained in detail in Ref. [1],  $a^2 = 2m\Delta\omega/R_e$ , where  $m$  is the mass of one fork's leg and  $R_e$  denotes its equivalent electrical resistance. The driving force per one leg of the fork is  $F = aU_0/2$ .

We have shown [1] that subject to a low drive, within a laminar regime, the resonance frequency  $f_0$  of the fork of density  $\rho_f$  and full width of the Lorentzian absorption curve  $\Delta f$  at half height (see an example of typical absorption and dispersion curves in the inset of Fig. 2) depend on the fluid density  $\rho$  and dynamic viscosity  $\eta$  as

$$\left(\frac{f_{0\text{vac}}}{f_0}\right)^2 = 1 + \frac{\rho}{\rho_f} \left( \beta + B \frac{S}{V} \sqrt{\frac{\eta}{\pi\rho f_0}} \right), \quad (1)$$

$$\Delta f = \frac{1}{2} \sqrt{\frac{\rho\eta f_0}{\pi}} CS \frac{(f_0/f_{0\text{vac}})^2}{\rho_f V}. \quad (2)$$

Here  $V = L_3 L_2 L_1$  is the volume of one fork's leg of length  $L_1$  and rectangular cross section  $L_3 L_2$ ,  $S = 2(L_3 + L_2)L_1$ . Equa-

tions (1) and (2) ignore the vacuum linewidth (at low temperature typically  $\Delta f_{\text{vac}} \approx 0.05$  Hz  $\ll \Delta f \approx 1-10$  Hz) and account fairly well for the behavior of the vibrating fork in fluids with known  $\rho$  and  $\eta$  if  $\beta$ ,  $B$ , and  $C$  are determined as fitting parameters [3].

The main result which we present here is our experimental observation of the transition from the laminar drag regime [characterized by the driving force  $F \propto U$ , where  $U$  is the peak velocity of the fork;  $f_0 \cong \text{const}$ ;  $\Delta f \cong \text{const}$ ; in accord with Eqs. (1) and (2)] to the turbulent drag regime (characterized by  $F \propto U^2$ ) in an oscillatory boundary layer flow [4].

The vibrating fork is an ideal tool for our investigations in that the same fork can be used in a rich variety of classical and quantum working fluids. Here we use  $^4\text{He}$ , offering three remarkable fluids of interest, primarily due to their extremely low values of kinematic viscosity,  $\nu = \eta/\rho$ , lowest of all known substances. Cryogenic helium gas in addition to its very low viscosity also allows an unprecedented flexibility, as its fluid properties can be easily tuned over many orders of magnitude by varying the temperature and/or pressure. Normal liquid helium (He I) is a Navier-Stokes fluid having normal boiling point at 4.2 K and existing (along the saturated vapor line, SVP) down to  $T_\lambda \approx 2.17$  K, below which it becomes superfluid and is usually referred to as He II. Properties of  $^4\text{He}$  are well known [5,6] and are easily tuneable by adjusting temperature and pressure *in situ* in the same pressure cell.

With cryogenic working fluids, such as He I or He II, care must be taken in order to prevent the extremely sensitive fork (typically  $Q \approx 10^5-10^6$  in vacuum at low temperature) from gathering solid particles of air or other contaminants. We therefore start measurement cycles with liquid helium under high pressure in the cell, so that for any subsequent measurement the amount of fluid in the pressure cell is either kept constant or decreases.

Our experimental protocol is based on recording families of resonant curves in various working fluids (i.e., in helium at various temperature and pressure) over six orders of magnitude of the drive—for such a wide dynamical range we need an additional attenuator and a step-up transformer. As shown in Fig. 2, on increasing the drive the Lorentzian shape of the absorption becomes distorted and the point of maxi-

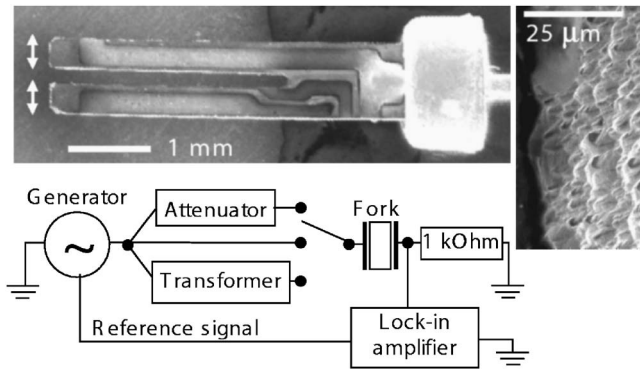


FIG. 1. The micrograph of the quartz tuning fork with the detail of its surface showing the typical surface roughness and the principal electrical circuitry used for measurements.

imum response  $f_{\max}$  shifts towards lower frequency [7].

In a steady classical flow past a submerged object, transition from laminar to turbulent drag occurs at some critical value of Reynolds number  $Re_{cr} = U_{cr} \ell / \nu$ , where  $U_{cr}$  denotes the critical flow velocity and  $\ell$  is a characteristic size of the object [8]. In a viscous flow due to an oscillating submerged body of the angular frequency of oscillation  $\omega = 2\pi f$  a new important length scale  $\delta = \sqrt{2\nu/\omega} = \sqrt{2\eta/\rho\omega}$  of the viscous penetration depth emerges. If  $\ell \ll \delta$  and, additionally, the Reynolds number  $U\ell/\nu$  is small, then the flow at any given instant can be regarded as steady—as if the body were moving uniformly with its instantaneous velocity. If, on the other hand,  $\ell \gg \delta$  and the amplitude of motion  $U/\omega \ll \ell$ , then the Reynolds number need not be small in order to neglect the nonlinear term in the Navier-Stokes equation. In a thin layer near the surface of the body the flow is rotational but in the rest of the fluid it is potential [9].

We suggest that in this case the transition from laminar to turbulent drag ought to be characterized by a critical Rey-

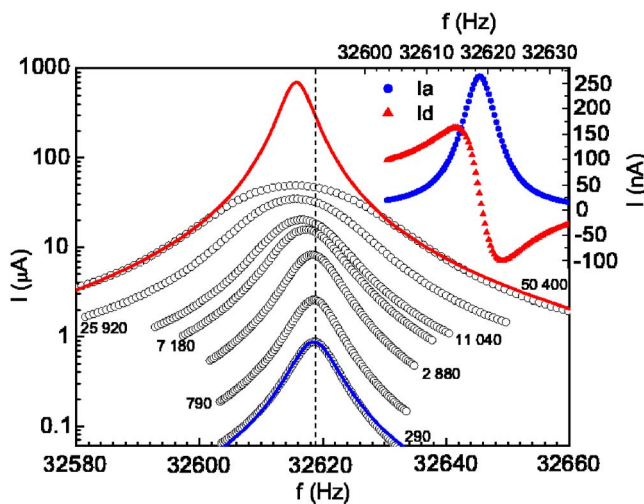


FIG. 2. (Color online) Left: The in-phase resonant response of the driven quartz fork vs applied frequency measured for various drive voltage levels (in  $mV_{rms}$ ) as indicated. The solid curves are Lorentzian fits to the data. The inset shows both absorption and dispersion curves for the drive level of  $290 mV_{rms}$ .

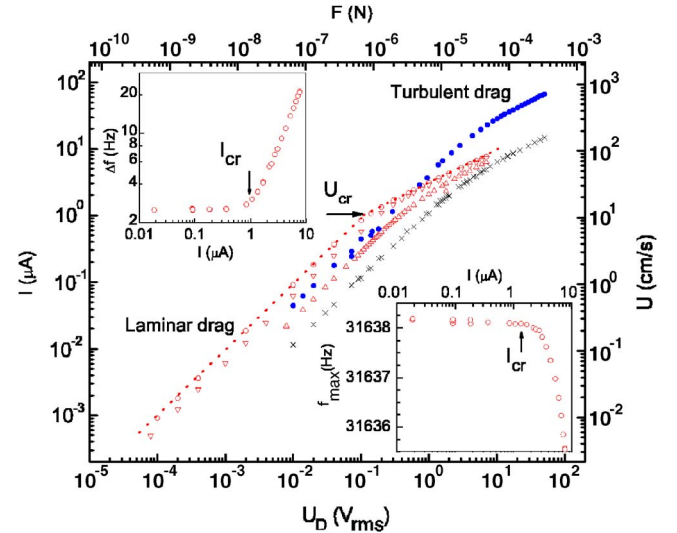


FIG. 3. (Color online) Transition from laminar to turbulent drag regime as detected by the vibrating quartz fork A2 in He I at 4.2 K and 18.6 bars ( $\times$ ), in He II at SVP at 1.37 K ( $\circ$ ), 1.61 K ( $\nabla$ ), 2.06 K ( $\Delta$ ), and in gaseous helium at 78 K and 10.05 bars ( $\bullet$ ). For conversion of measured electrical quantities  $U_D$  and  $I$  to  $F$  and  $U$ , see [1]. The insets show the width  $\Delta f$  of the in-phase resonance response (top) and the frequency of maximum response  $f_{\max}$  (bottom) vs measured current, both being constant in a linear regime. Increase of  $\Delta f$  and decrease of  $f_{\max}$  indicate an onset of the turbulent drag regime.

nolds number based on the penetration depth:

$$Re_{cr}^{\delta} = U_{cr} \delta / \nu. \quad (3)$$

It immediately follows that the critical velocity ought to scale as  $U_{cr} \propto \sqrt{\nu\omega}$ .

For full description of oscillatory flows, besides the Reynolds number one needs to define an additional dimensionless number such as the Strouhal number  $St = U\tau/\ell$  [9], where  $\tau = 2\pi/\omega$  is a characteristic time. Note that if one assumes that the characteristic length scale is the penetration depth, Reynolds and Strouhal numbers become equal (except for a numerical constant of  $\pi$ ). Consequently, the crossover from the laminar to turbulent drag can be described by the Reynolds number  $Re_{cr}^{\delta}$  alone.

Note that with our quartz tuning fork oscillating at about 32 kHz (despite covering six orders of magnitude of  $F$  resulting in five orders of magnitude of  $U$ ) we always operate in the limit  $U/\omega \leq 20 \mu m \ll \ell \approx 400 \mu m \gg \delta \leq 4.3 \mu m$ . The velocity when the amplitude of oscillation would reach the thickness of the fork's leg would be  $U \approx 80 m/s$  and cannot be reached in practice—the fork mechanically breaks at velocities of order of a few m/s [10].

In most cases, however, the attainable velocity of the fork is high enough to comfortably observe the transition from laminar to turbulent drag regime (see Fig. 3). It is clearly marked as a change in the velocity vs drive slope as well as by the onset of increase in observed  $\Delta f$  or an onset of decrease of  $f_{\max}$ . Experimentally, we define the critical velocity  $U_{cr}$  as a crosspoint of fitted linear and square-root velocity vs

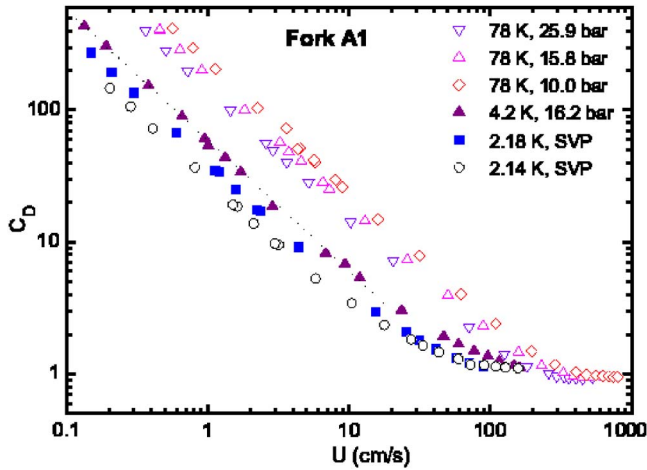


FIG. 4. (Color online) The drag factor  $C_D$  plotted vs the peak velocity  $U$  of the fork. Measurements in helium gas, in normal liquid He I as well as in superfluid He II close to the transition temperature, are shown at conditions as indicated. The dotted line is included to appreciate an expected  $C_D \propto 1/U$  behavior in laminar regime.

driving force dependence, neglecting the data points where rounding in the vicinity of  $U_{cr}$  takes place.

The universal crossover behavior is even better displayed in a nondimensional way in Fig. 4, where we plot the velocity dependence of the classical drag factor defined as  $C_D = 2F/\rho AU^2$ , where  $A = L_1 L_2$  is the projected area of the fork's leg. As a numerical example, for the fork A1 (see Fig. 4)  $C_D = 1 \pm 0.2$  over two decades of  $\nu$  and more than a decade of  $\rho$ , as measured in classical fluids He I and He gas at various applied pressures.

Our data obtained in classical viscous fluids (covering two orders of magnitude of  $\nu$  and thus demonstrating the usefulness of cryogenic helium for laboratory fluid dynamical research) displayed in Fig. 5 verify the scaling  $U_{cr} \propto \sqrt{\nu\omega}$  in the limit  $\ell \gg \delta$  [11]. In order to stress that our results do not depend on the particular fork, we show our results obtained with two nominally identical forks A1 and A2 and with a bigger fork B1 [2]. The critical value of  $Re_{cr}^\delta$  is about 5 [12] and varies slightly from fork to fork (within about 20%), but the scaling for each individual fork holds. Thus for oscillatory flow due to a vibrating object, in the limit  $U/\omega \ll \ell \gg \delta$ , the characteristic length scale is not the size of the object, but the viscous penetration depth.

To better appreciate our experimental results, it is instructive to consider an analytically tractable example of a viscous flow due to an oscillating hydrodynamically smooth sphere. In a laminar regime, the drag force acting upon a sphere of radius  $R$  is given [9],  $F_{lam} = \lambda U = 6\pi\eta R(1 + R/\delta)U$ . For the turbulent drag regime we adopt  $F_{turb} = \gamma U^2 = C_D \rho \pi R^2 U^2 / 2$ . Assuming that the transition occurs when these forces become equal in a limit of high frequency ( $R \gg \delta$ ) we arrive at

$$U_{cr} = \frac{\lambda}{\gamma} \cong \frac{6\sqrt{2}}{C_D} \sqrt{\nu\omega} \approx 21\sqrt{\nu\omega}. \quad (4)$$

Here we assumed that for a smooth sphere  $C_D \approx 0.4$ . In He I at the saturated vapor curve just above the superfluid transi-

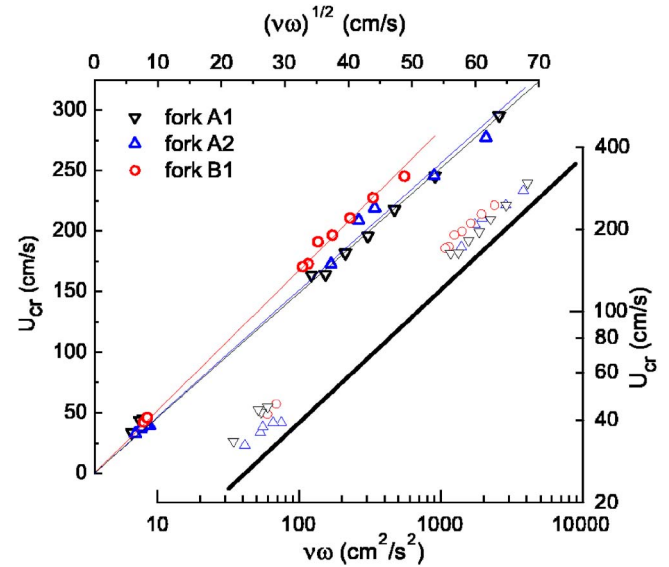


FIG. 5. (Color online) The critical velocity at which transition from laminar to turbulent drag occurs for three different forks A1, A2, and B1 [2] in classical fluids (data points obtained using He I in the temperature range  $2.2 < T < 4.2$  K and He gas at 78 K at ambient and elevated pressure up to 30 bars) plotted vs  $\sqrt{\nu\omega}$ . The solid lines represent the best linear fit that includes the (0,0) point (top). This scaling is confirmed by comparison with the thick solid line in the logarithmic plot (bottom); the fitted power laws for the three forks yield  $0.48 \pm 0.04$ .

tion this would give a critical velocity of about 1.3 m/s, about four times higher than we observe for the oscillating fork. It seems therefore that for submerged oscillating bodies of arbitrary shape (such as, e.g., quartz fork) Eq. (4) generally holds, with appropriate numerical values of  $\lambda$  and  $\gamma$ . Here we assume that  $\ell \gg \delta$ . The expression for  $F_{lam}$  suggests that there ought to be a crossover from a regime where  $\ell \ll \delta$  to  $\ell \gg \delta$ . It is an interesting question if such a crossover is always present in boundary layer flows due to bodies of various forms.

The example of a sphere is certainly too simple to account for any details within the crossover region, such as instability against Taylor-Görtler vortices [13]. We have chosen this simplest example of a sphere having in mind that the flow over the tip of the fork is inherently three dimensional. Taking into account the surface roughness (see Fig. 1) and the fact that the tip of the fork's leg is partly ground off by the manufacturer to adjust the desired room-temperature frequency, it is hardly possible to accurately describe the flow analytically or even numerically. It seems, nevertheless, that the underlying physics of a crossover from laminar to turbulent drag regime is captured and such a comparison is useful.

We have extended our measurements and analysis to a quantum fluid—He II. One might expect a very different behavior here, as it is well known that He II displays the two-fluid phenomena and circulation in its superfluid component is quantized. It is remarkable therefore that in He II we observe similar drive dependencies as in He I and He gas. In particular, no appreciable change in the measured quantities is observed when crossing  $T_\lambda$  (see Figs. 3 and 4). On decreasing the temperature of He II along the saturated vapor

curve further, however, the crossover becomes gradually sharper and across the transition region the drag coefficient displays additional pronounced features. We observe neither irregularities nor any hysteretic phenomena down to about 1.3 K, although we have especially searched for them. Such features have been commonly observed with oscillating wires [14], spheres [15], or grids [16], but in most cases at lower temperatures. Due to space restriction, we postpone a detailed account and analysis of He II measurements to a later publication; here we restrict ourselves to merely stating their main features.

To conclude, we have experimentally confirmed that a critical velocity for the crossover from laminar to turbulent drag regime in a viscous flow due to an oscillating quartz fork in the limit  $U/\omega \ll \ell \gg \delta$  scales as  $U_{cr} \propto \sqrt{\nu\omega}$  over at

least two decades of kinematic viscosity. Taking into account the geometrical shape of the tip of the fork's leg and its surface roughness, this result strongly suggests that for such an oscillatory flow the characteristic length scale is not the size of the object, but the viscous penetration depth  $\delta = \sqrt{2\nu/\omega}$ .

The authors appreciate the technical help of T. V. Chagovets, L. Doležal, M. Rotter, F. Soukup, and P. Vacek, stimulating discussion with many colleagues, especially D. Charalambous, V. B. Eltsov, R. Hanninen, J. Hosio, M. Krusius, P. V. E. McClintock, J. J. Niemela, W. Schoepe, P. Skyba, K. R. Sreenivasan, W. F. Vinen, H. Yano, and thank J. Pešička for providing the fork micrographs. This research was supported by research plans MS 0021620834, AVOZ 10100520, and by GAČR under 202/05/0218.

- 
- [1] R. Blaauwgeers *et al.*, Quartz Tuning Forks—Thermometers, Pressure- and Viscometers for Cryogenic Fluids, *J. Low Temp. Phys.*, Nos. 5/7 (2007), in e-print, cond-mat/0608385.
- [2] Forks specified as type DT26 (A1,A2) and DT38 (B1) used in this work have been produced by Fronter Electronics, China, www.chinafronter.com
- [3] This approach does not take into account a steady secondary flow through the action of viscosity in the boundary layer (e.g., streaming [8]) and  $\beta$  therefore weakly depends on the geometry of the surrounding container.
- [4] This transition in He II was independently observed by J. Hosio, V. B. Eltsov, and M. Krusius in LTL Helsinki; (private communication).
- [5] R. D. McCarty, Technical Note 631, National Bureau of Standards, Gaithersburg, Maryland, 1972; V. D. Arp, R. D. McCarty, "The Properties of Critical Helium Gas," Technical Report, University of Oregon, 1998.
- [6] R. J. Donnelly and C. F. Barenghi, *J. Phys. Chem. Ref. Data* **27**, 1217 (1998).
- [7] We do not use the term resonant frequency as above the transition the response curve ceases to be of the Lorentzian form, as illustrated in Fig. 2.
- [8] H. Schlichting and K. Gersten, *Boundary-Layer Theory* (Springer, New York, 1996).
- [9] L. D. Landau and E. M. Lifshitz, *Fluid Mechanics* (Pergamon, New York, 1959).
- [10] An additional factor that has to be taken into account is cavitation that often occurs when working in liquid helium at or near the saturated vapor pressure and the fork oscillates at large amplitude. Its signature is an irregular shift of the resonant frequency to values between those of the liquid and gaseous phases. Our measurements of heterogeneous cavitation in He I and He II will be reported and discussed in detail elsewhere.
- [11] Note that this scaling differs from that found using the transversally oscillating cylinders, see T. Sarpkaya, *J. Fluid Mech.* **165**, 61 (1986), and references therein.
- [12] Comparison with other oscillating objects is not straightforward, as the flow becomes enhanced while passing the sharp edges of the fork and due to surface roughness.
- [13] S. R. Otto, *J. Fluid Mech.* **239**, 47 (1992).
- [14] M. Morishita, T. Kuroda, A. Sawada, and T. Satoh, *J. Low Temp. Phys.* **76**, 387 (1989); H. Yano *et al.*, *ibid.* **138**, 561 (2005); (private communication).
- [15] J. Jäger, B. Schuderer, and W. Schoepe, *Phys. Rev. Lett.* **74**, 566 (1995).
- [16] H. A. Nichol, L. Skrbek, P. C. Hendry, and P. V. E. McClintock, *Phys. Rev. Lett.* **92**, 244501 (2004); *Phys. Rev. E* **70**, 056307 (2004); D. Charalambous *et al.*, *ibid.* **74**, 036307 (2006).